Nikolay Ivanov Kolev

Multiphase Flow Dynamics

2 MECHANICAL INTERACTIONS

Fourth Edition

Springer

Multiphase Flow Dynamics 2

Nikolay Ivanov Kolev

Multiphase Flow Dynamics 2

Mechanical Interactions

Springer

Author

Dr. Nikolay Ivanov Kolev
Möhrendorferstr. 7
91074 Herzogenaurach
Germany
E-mail: Nikolay.Kolev@herzovision.de

ISBN 978-3-642-20597-2 e-ISBN 978-3-642-20598-9

DOI 10.1007/978-3-642-20598-9

Library of Congress Control Number: 2011934149

Typeset & Cover Design: Scientific Publishing Services Pvt. Ltd., Chennai, India.

Printed on acid-free paper

9 8 7 6 5 4 3 2 1

springer.com

To Iva, Rali and Sonja with love!

Venice, July. 2004, Nikolay Ivanov Kolev, 36× 48cm oil on linen

Nikolay Ivanov Kolev, PhD, DrSc
Born 1.8.1951, Gabrowo, Bulgaria

Summary

This monograph presents theory, methods, and practical experience for the description of complex transient multiphase processes in arbitrary geometrical configurations. It is intended to aid applied scientists and practicing engineers to better understand natural and industrial processes containing dynamic evolutions of complex multiphase flows. The book is also intended to be a useful source of information for students in the high semesters and in PhD programs.

This monograph consists of five volumes:

Vol. 1 Fundamentals, 4th ed., (14 Chapters and 2 Appendices), 782 pages,
Vol. 2 Mechanical interactions, 4th ed., (11 Chapters), 364 pages,
Vol. 3 Thermal interactions, 4th ed., (16 Chapters), 678 pages,
Vol. 4 Turbulence, gas absorption and release by liquid, diesel fuel properties, 2nd ed., (13 Chapters), 328 pages
Vol. 5 Nuclear Thermal Hydraulics, 2nd ed., (17 Chapters), 848 pages

In Volume 1 the concept of three-fluid modeling is presented in detail "from the origin to the applications." This includes derivation of local volume- and time-averaged equations and their working forms, development of methods for their numerical integration and finally finding a variety of solutions for different problems of practical interest.

Special attention is paid in Volume 1 to the link between the partial differential equations and the constitutive relations called closure laws without providing any information on the closure laws.

Volumes 2 and 3 are devoted to these important constitutive relations for mathematical description of the mechanical and thermal interactions. The structure of the volumes is in fact a state-of-the-art review and selection of the best available approaches for describing interfacial transfer processes. In many cases the original contribution of the author is incorporated in the overall presentation. The most important aspects of the presentation are that they stem from the author's long years of experience developing computer codes. The emphasis is on the practical use of these relationships: either as stand-alone estimation methods or within a framework of computer codes.

Volume 4 is devoted to the turbulence in multiphase flows.

The nuclear thermal hydraulic field is the science providing knowledge about the physical processes occurring during transfer of fission heat released in structural materials due to nuclear reactions into the environment. Along its path to the environment the thermal energy is organized to provide useful mechanical work or useful heat or both. Volume 5 is devoted to nuclear thermal hydraulics. In a way this is the most essential application of multiphase fluid dynamics in the analysis of steady and transient processes in nuclear power plants.

In particular, **Volume 2** contains information on how to describe the flow patterns and the specific mechanical interactions between the velocity fields in flight.

In Chapter 1 velocity scales and definitions frequently used in constructing flow pattern maps are given. The flow regime transition criteria in transient multiphase flows are presented for the cases of pool flow, adiabatic flow, channel flow in vertical pipes, channel flow in inclined pipes, heated channels, porous media, and particles in film boiling. Additional information is presented for flow pattern in rod bundles. The idea of flow pattern boundaries depending on the transient evolution of the particle number and particle size is presented.

Chapter 2 collects updated information about modeling the drag forces on a single bubble, a family of particles in a continuum, droplets in a gas, solid particles in a gas in the presence of a liquid, solid particles in a liquid in the presence of a gas, solid particles in a free-particle regime, solid particles in bubbly flow, solid particles in a densely packed regime, annular flow, inverted annular flow, stratified flow in horizontal or inclined rectangular channels and stratified flow in horizontal or inclined pipes. Constitutive relationships for the lift- and virtual mass forces are provided. Discussion is provided for the uncertainty of the film-gas forces.

Chapter 3 presents information about the friction pressure drop in single- and multiphase flow. Additionally, Rehme's method for computation of pressure drop of flow in channels with arbitrary cross section, pressure drop in rod bundles for axial and cross flow, and pressure drop at spacers in rod bundles in nuclear reactors is given.

Historically algebraic correlations for describing the velocity difference preceded the development of interfacial interaction models. The large number of empirical correlations for the diffusion velocities for algebraic slip models for two- and three-phase flows is provided in Chapter 4.

Chapter 5 is devoted to entrainment in annular two-phase flow. It has been updated with recent information. Discussion is provided on entrainment increase in boiling channels, residual film thickness during dry out, and entrainment increase due to obstacles. Estimation of the uncertainty of the existing state-of-the-art is performed based on the dry-out process in a boiling channel.

Chapter 6 is devoted to deposition in annular two-phase flow. It has been updated with recent information. Discussion is provided on the influence of nucleate boiling inside the film and on heat transfer due to the bouncing of the droplets onto the hot wall. Estimation of the uncertainty of the existing state-of-the-art is performed based on the dry-out process in a boiling channel.

Chapter 7 gives an introduction to fragmentation and coalescence dynamics in multiphase flows. Acceleration-induced droplet and bubble fragmentation is described in Chapter 8. Chapter 9 is devoted to turbulence-induced particle fragmentation and coalescence and Chapter 10 to liquid and gas jet disintegration. Chapter 11 presents the state-of-the-art on the fragmentation of melt in a coolant, covering a variety of aspects.

29.12.2010 Nikolay Ivanov Kolev
Herzogenaurach

Table of Contents

1 Flow regime transition criteria

This chapter presents a review of the existing methods for identification of flow patterns in two-phase flow in pools, adiabatic and nonadiabatic channels, rod bundles and porous structures. An attempt is made to extend this information to be applicable in three-phase flow modeling. In addition the influence of the dynamic fragmentation and coalescence of flow regimes is introduced.

1.1 Introduction

Transient multiphase flows with temporal and spatial variation of the volumetric fractions of the participating phases can be represented by *sequences* of geometric *flow patterns* that have some characteristic length scale. Owing to the highly random behavior of the flow in detail, the number of flow patterns needed for this purpose is very large. Nevertheless, this approach has led to some successful applications in the field of multiphase flow modeling. Frequently modern mathematical models of *transient flows* include, among others, the following features:

1. Postulation of a limited number of idealized flow patterns, with transition limits as a function of local parameters for *steady-state* flow (e.g., see Fig. 1.1);
2. Identification of one of the postulated idealized *steady-state* flow patterns for each time step;
3. Computation of a characteristic *steady-state length scale of the flow patterns* (e.g., bubble or droplet size) in order to address further constitutive relationships for interfacial heat, mass, and momentum transfer.

Various transfer mechanisms between mixture and wall, as well as between the velocity fields, depend on the flow regimes. This leads to the use of regime-dependent correlations for modeling of the interfacial mass, momentum, and energy transfer. The transfer mechanisms themselves influence strongly the flow pattern's appearance. That is why the first step of the coupling between the system PDEs (Partial differential equations) and the correlations governing the transfer mechanisms is the flow regime identification.

We distinguish between flow patterns appearing in *pool* flow and in *channel* flow. In pool flow, $\gamma_v = 1$, there is no influence of the walls on the flow pattern. In channel flows characterized by $\gamma_v < 1$, however, this influence can be very strong resulting in patterns like film flow, slug flow etc.

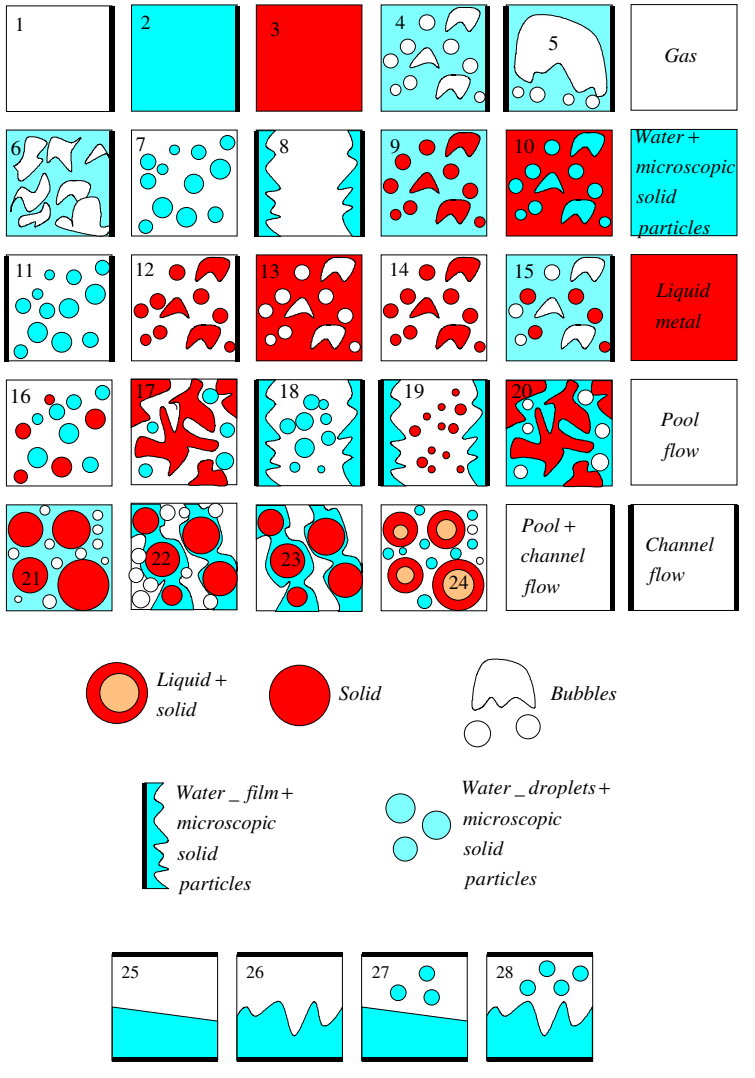

Fig. 1.1 Multiphase flow patterns

Some flow patterns can be trivially identified by knowing only the values of the local volume fractions of the fields, α_l, and the consistency of the fields that is C_{li}, for example the single-phase flows or flows consisting of three velocity fields with an initially postulated structure. For two interpenetrating velocity fields additional information is necessary to identify the flow pattern. There are analytical and experimental arguments for flow pattern identification which will

be considered here. The emphasis of this chapter is on how dynamics influence the transitions from one flow pattern into another.

1.2 Pool flow

In pool flows we distinguish two main flow patterns: continuous liquid and continuous gas, and one intermediate between them. Next we discuss the conditions for existence of bubble flow. We will realize that dynamic fragmentation and coalescence will have an influence on the transition criterion through the bubble size.

Bubbly flow: The existence of bubbly flow in pools is discussed in this section.

Nonoscillating particles: Consider equally sized spherical particles forming a rhomboid array. The average distance between the centers of two adjacent particles with diameter D_d and volumetric fraction α_d is then

$$\Delta\ell_d = D_d\left(\frac{\pi}{6}\frac{\sqrt{2}}{\alpha_d}\right)^{1/3}. \tag{1.1}$$

Here *d* stands for disperse. The *nonoscillating* particles will touch each other if

$$\Delta\ell_d = D_d. \tag{1.2}$$

This happens for a volume fraction of

$$\alpha_d = \frac{\pi}{6}\sqrt{2} \approx 0.74, \tag{1.3}$$

which is sometimes called in the literature the *maximum packing density* volume concentration. This consideration leads to the conclusion that bubble flow cannot exist for

$$\alpha_1 > 0.74, \tag{1.4}$$

and vice versa droplet flow cannot exist for

$$\alpha_1 < 0.26. \tag{1.5}$$

Oscillating particles: Oscillating particles will touch each other occasionally at larger average distance. This means that in strongly turbulent flows the existence of bubble flow should be expected to be limited by smaller volume fractions. In fact turbulent bubble flows in nature and technical facilities are observed up to

$$\alpha_1 < 0.25 \text{ to } 0.3, \tag{1.6}$$

Taitel et al. (1980), *Radovich* and *Moissis* (1962), see *Mishima* and *Ishii* (1984). If the mean free path length of the oscillating particles is ℓ_d^t the sphere of influence of this particle is $D_d + \ell_d^t = D_d\left(1+\ell_d^t/D_d\right)$. In this case the particles may touch each other if

$$D_d\left(1+\ell_d^t/D_d\right) = D_d\left(\frac{\pi}{6}\frac{\sqrt{2}}{\alpha_d}\right)^{1/3}, \tag{1.7}$$

or

$$\alpha_d = \frac{\pi}{6}\sqrt{2}\,/\left(1+\Delta\ell_d^t/D_d\right) < 0.74\,, \tag{1.8}$$

and consequently

$$\ell_d^t/D_d > 0.44 \text{ to } 0.35\,. \tag{1.9}$$

The influence of the particle size on the flow regime transition: Brodkey (1967) shows that bubbles with radii smaller than

$$D_{1,\text{solid like}} = 0.63\sqrt{\frac{2\sigma_2}{g\Delta\rho_{21}}} \approx 0.89\lambda_{RT}\,, \tag{1.10}$$

where λ_{RT} is the *Raleigh-Taylor* wavelength defined as follows

$$\lambda_{RT} = \sqrt{\frac{\sigma_2}{g\Delta\rho_{21}}}\,, \tag{1.11}$$

behave as a solid sphere and the coalescence is negligible. This argument was used by *Taitel* et al. (1980) to explain the existence of bubble flow in regions up to

$$\alpha_1 < 0.54\,, \tag{1.12}$$

if strong liquid turbulence destroys bubbles to dimensions

$$D_1\left(\varepsilon_2,...\right) < D_{1,\text{solid like}} \tag{1.13}$$

where ε_2 is the dissipation rate of the turbulent kinetic energy of the liquid.

Conclusions:

1) In the concept of modeling dynamic fragmentation and coalescence, bubble flow is defined if we have at least one bubble in the volume of consideration, Vol_{cell}, that is

$$n_1 Vol_{cell} > 1\,, \tag{1.14}$$

otherwise both phases are continuous. This is the trivial condition. Here n_1 is the number of bubbles per unit mixture volume.

2) For small bubble sizes, $D_1(\varepsilon_2,...) < D_{1,solid\ like}$, the bubbles behave as solid spheres and the coalescence probability is dramatically reduced. In this case bubble flow exists up to

$$\alpha_{1,B-Ch} = 0.54 . \tag{1.15}$$

3) For larger bubble sizes, $D_1(\varepsilon_2,...) > D_{1,\text{solid like}}$, the transition between bubble and churn-turbulent flow happens between

$$\alpha_{1,B-Ch} \approx 0.25 \text{ and } 0.54 . \tag{1.16}$$

The size at which the lower limit holds is not exactly known. Assuming that this size is governed by a critical *Weber* number equal to 12 and using the bubble rise velocity in the pool as computed by *Kutateladze*

$$V_{1Ku} = \sqrt{2}\left[g\sigma_2 (\rho_2 - \rho_1)/\rho_2^2 \right]^{1/4} ,$$

we obtain 6-times λ_{RT}. A linear interpolation between these two sizes gives

$$\alpha_{1,B-Ch} = 0.54 - 0.0567\left(D_1/\lambda_{RT} - 0.89\right) . \tag{1.17}$$

The dependence of this transition criterion on the bubble size is remarkable. Modeling dynamic bubble size evolution gives different regime transition boundaries for different bubble sizes at the same gas volume fraction.

4) Churn-turbulent flow exists between

$$0.54 < \alpha_1 < 0.74 . \tag{1.18}$$

Note that the upper limit of the churn-turbulent flow, $\alpha_{1,Ch-A} = 0.74$, seems to be a function of the local *Mach* number. The higher the local *Mach* number, the higher the upper limit due to the increasing turbulence. This consideration is supported by the position of the slip maximum as a function of the gas volume fraction in critical flow as measured by for example *Deichel* and *Winter* (1990). The investigation of *Ginsberg* et al. (1979) of flow behavior of volume-heated boiling pools shows that for fast transients the limit between bubble and churn-turbulent flow and dispersed flow is higher. Thus, one can assume that the upper limit is

$$\alpha_{1,Ch-A} = 0.74 + Ma\left(0.92 - 0.74\right) = 0.74 + 0.18Ma . \tag{1.19}$$

In accordance with this consideration, very slow flows do not have churn turbulent regimes and bubble flow goes directly into disperse droplet flow with increasing gas volume fraction.

1.3 Adiabatic flows

Boundaries between flow-patterns are frequently expressed as a function of important velocity scales. Such velocity scales are the so-called velocity of a *Taylor* bubble and the *Kutateladze* velocity. Next we briefly describe how they appear in the two-phase flow analysis.

1.3.1 Two important velocity scales

Velocity of Taylor bubble: For a free-rising bubble in liquid and free-falling droplet in a gravitational field as shown in Fig. 1.2 the drag force is equal to the buoyancy force

$$c_{cd}^{d}\frac{1}{2}\rho_c\left(w_c-w_{d\infty}\right)^2\pi D_{d\infty}^2/4=\left(\pi D_{d\infty}^3/6\right)g\Delta\rho_{dc}\,.$$

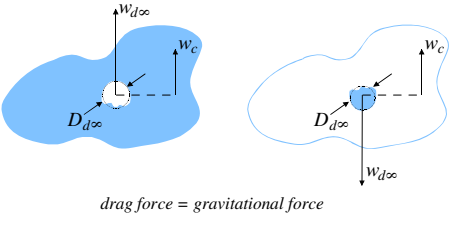

Fig. 1.2 Free-falling droplet in a gravitational field and free-rising bubbles in liquid

For $c_{cd}^{d}\approx const$ we have

$$\Delta w_{dc}=\frac{1}{\sqrt{3c_{cd}^{d}}}\Delta w_{dc,RT}\approx const\,\Delta w_{dc,RT}\,.$$

The so-defined characteristic velocity is called the *Taylor*-velocity

$$\Delta w_{dc,RT}=\sqrt{D_{d\infty}g\frac{\Delta\rho_{dc}}{\rho_c}}\,.$$

For a *slug* in vertical pipes (see Fig. 1.3) where $D_{d\infty}\approx D_h$, the slug rise velocity was experimentally found by *Dimitresku* (1943) and *Davies* and *Taylor* (1950) to be dependent on the pipe diameter

$$\Delta w_{12}=0.35\Delta w_{12,RT}\,.$$

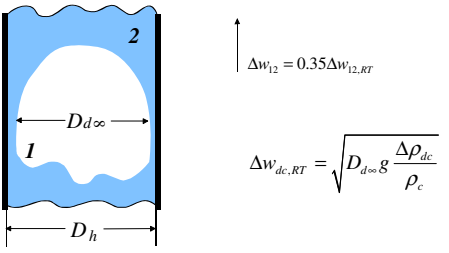

Dimitresku (1943), Davies und Taylor (1950)

Fig. 1.3 Free-rising gas slug in pipe

Kutateladze velocities: For large bubbles where the size is comparable to the *Rayleigh-Taylor* instability wavelength for the case where gas and liquid are interpenetrating due to gravity

$$D_{d\infty} \approx \lambda_{RT} = \left[\sigma_d / \left(g\Delta\rho_{dc}\right)\right]^{1/2}.$$

In this case the free-rising bubble velocity in a pool or the free-falling droplet velocity in a gas, see Fig. 1.4, is

$$\Delta w_{dc} = \frac{1}{\sqrt{3c_{cd}^d}}\left(\frac{\sigma_d g\Delta\rho_{dc}}{\rho_c^2}\right)^{1/4} \approx \left(\sqrt{2}\ to\ 1.7\right)\left(\frac{\sigma_d g\Delta\rho_{dc}}{\rho_c^2}\right)^{1/4} = \left(\sqrt{2}\ to\ 1.7\right)\Delta w_{dc,Ku}.$$

Here

$$\Delta w_{dc,Ku} = \left(\frac{\sigma_d g\Delta\rho_{dc}}{\rho_c^2}\right)^{1/4}$$

is called the *Kutateladze* velocity, see *Kutateladze* (1951). Note that

$$\frac{\Delta w_{dc,Ku}}{\Delta w_{dc,RT}} = \left(\frac{\lambda_{RT}}{D_{d\infty}}\right)^{1/2}.$$

One will immediately recognize the importance of the above-discussed velocity scale if the phenomenon of flooding has to be simply described. Flooding is a limit to counter-current flow where the gas phase is flowing upwards and the liquid phase is stagnating.

Flooding in vertical channels with large sizes: For large pipes the flow pattern is schematically presented in Fig. 1.5. *Kutateladze* (1951) found that the condition for gas stagnation after injection through a horizontal perforated plate in water is

$\left[\alpha_1 w_{10}/\left(\sqrt{2}\Delta w_{21,Ku}\right)\right]^{1/2} = const$. The constant is reported by *Pushkina* and *Sorokin* (1969) to be 1.79,

$$\left(\alpha_1 w_1\right)_{\lim} = 3.2\sqrt{2}\Delta w_{21,Ku} .$$

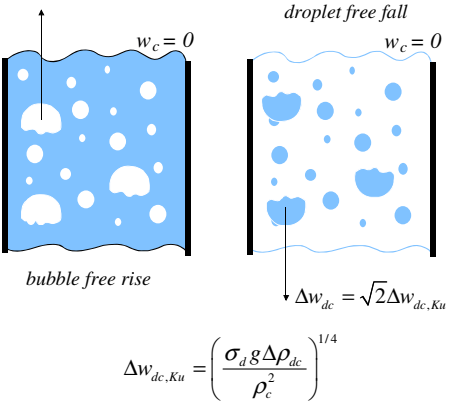

Fig. 1.4 Free-rising bubbles and free-falling droplets

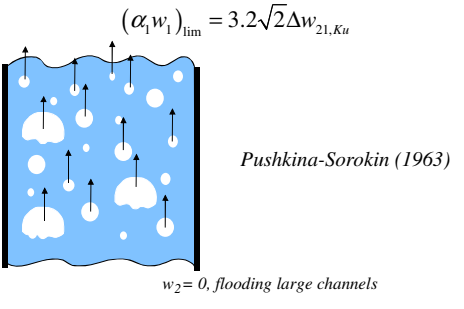

Fig. 1.5 Flooding in large pipes: the gas phase blocks the down flow of the liquid

Tien et al. (1979) extended the validity of the *Pushkina* and *Sorokin* correlation to pipe diameters of different sizes as follows

$$\left[\alpha_1 w_{10}/\left(\Delta w_{21,Ku}\right)\right]^{1/2} + c_1\left[\alpha_2 w_{20}/\left(\Delta w_{12,Ku}\right)\right]^{1/2} = c_2 \tanh\left[c_3\left(D_h/\lambda_{RT}\right)^{1/4}\right],$$

where $c_1 = 0.65$ to 0.8 , $c_2 = 1.79$ to 2.1 , $c_3 = 0.8$ to 0.9 .

Flooding in vertical channels with small sizes: *Wallis* (1969, p. 338), proposed the following relation defining the so-called counter-current flow limitation

$$\left[\frac{\alpha_1 w_{10}}{\sqrt{D_h g \dfrac{\Delta\rho_{21}}{\rho_1}}}\right]^{1/2} + \left[\frac{(1-\alpha_1) w_{20}}{\sqrt{D_h g \dfrac{\Delta\rho_{21}}{\rho_2}}}\right]^{1/2} = C\,,$$

where $C = 0.775$. For sharp-ended pipes, $C = 0.88$ $j_{20}^{*} < 0.3$, $C = 1$ otherwise, *Hewitt* and *Wallis* (1963). There are a variety of sophistications of this expression in the literature but its main structure remains the same. In a cross section where the outflowing liquid volume flow is equal to the inflowing gas flow, $\alpha_1 w_{10} = (1-\alpha_1) w_{20}$, see Fig. 1.6 left, we have

$$\alpha_1 w_{10} = (1-\alpha_1) w_{20} = C^2 \frac{\left(D_h g \Delta\rho_{21}\right)^{1/2}}{\left(\rho_1^{1/4} + \rho_2^{1/4}\right)^2}\,.$$

The relation between the flooding condition and the slug velocity was found by *Whalley* (1987) after setting $\alpha_1 w_{10} = 0.35 \Delta w_{12,RT}$. The result is

$$C = \sqrt{0.35}\left(1 + \rho_1^{1/4} / \rho_2^{1/4}\right).$$

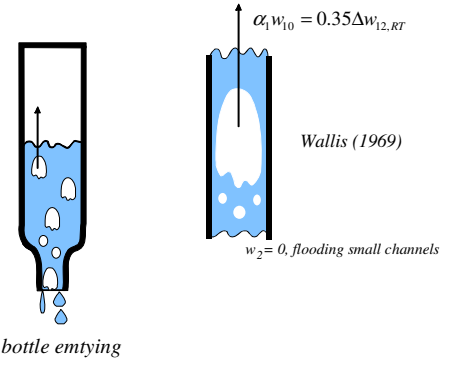

Fig. 1.6 Flooding in small channels

1.3.2 Channel flow – vertical pipes

For vertical pipe flows the following regime boundaries are defined:

Bubble flow: As for the pool flow, in the concept of modeling dynamic fragmentation and coalescence, bubble flow is defined if we have at least one bubble in the volume of consideration, Vol_{cell}, that is

$$n_1 Vol_{cell} > 1, \tag{1.20}$$

otherwise both phases are continuous.

Figure 1.7 indicates that the *Rayleigh-Taylor* instability wavelength λ_{RT} is the appropriate scale for distinguishing whether the pipe diameter is small or large.

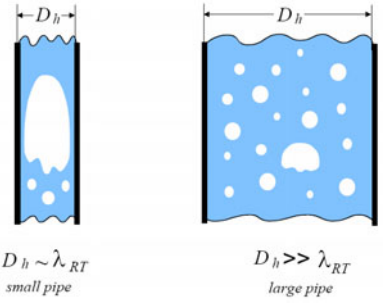

Fig. 1.7 Criterion for distinguishing between small and large channels

Bubble flow exists in the region

$$0 < \alpha_1 < \alpha_{1,bubble\ to\ slug} \quad \text{and} \quad D_h > D_{h,slug}, \tag{1.21}$$

where

$$D_{h,slug} = 19 \frac{\Delta\rho_{21}}{\rho_2} \lambda_{RT}, \quad \textit{Taitel} \text{ et al. (1980)}, \tag{1.22}$$

$$\alpha_{1,bubble\ to\ slug} = 0.54 \ \text{ for } \ D_1(\varepsilon_2,...) < 0.89\lambda_{RT}, \tag{1.23}$$

$$\alpha_{1,bubble\ to\ slug} = 0.54 - 0.0567\left(D_1/\lambda_{RT} - 0.89\right) \ \text{ for } \ 0.89\lambda_{RT} < D_1(\varepsilon_2,...) < 6\lambda_{RT}, \tag{1.24}$$

$$\alpha_{1,bubble\ to\ slug} \approx 0.25 \ \text{ for } \ D_1(\varepsilon_2,...) \geq 6\lambda_{RT}. \tag{1.25}$$

Slug flow: Slug flow is defined as a train of large bubbles followed by mixtures of small bubbles and liquid or liquid only. The slug regime is never stationary. Slug flow exists if

$$D_h < D_{h,slug} \tag{1.26}$$

or if

$$D_h > D_{h,slug} \ \text{ and } \ \alpha_{1,bubble\ to\ slug} < \alpha_1 < \alpha_{1,slug\ to\ churn}. \tag{1.27}$$

This condition reflects the fact that slug flow can be transformed into churn-turbulent flow if the gas volume fraction averaged over the entire pipe length is larger than those in the slug bubble section only. The gas volume fraction in the slug bubble section only is

$$\alpha_{1,slug\ to\ churn} = 1 - 0.813 \left\{ \frac{(C_0 - 1)\ |j| + 0.35\ V_{TB}}{|j| + 0.75\ V_{TB} b_1} \right\}^{0.75}, \tag{1.28}$$

Mishima and *Ishii* (1984). The drift flux distribution coefficient for slug flow is

$$C_0 = 1.2, \tag{1.29}$$

the slug (*Taylor* bubble) rising velocity is

$$V_{TB} = \sqrt{\frac{\rho_2 - \rho_1}{\rho_2} g D_h}, \tag{1.30}$$

the mixture volumetric flux is

$$j = \alpha_1 V_1 + (1 - \alpha_1) V_2, \tag{1.31}$$

and

$$b_1 = \left(\frac{\rho_2 - \rho_1}{\eta_2^2 / \rho_2} g D_h^3 \right)^{1/18}. \tag{1.32}$$

The correlation contains the length of the *Taylor* bubble

$$\sqrt{2 \ell_{TB} \Delta\rho_{21} g / \rho_2} = |j| + 0.75\ V_{TB} b_1. \tag{1.33}$$

The error for computing ℓ_{TB} is $\pm 100\%$. Thus, air-water flow in a pipe with diameter $D_h = 0.027m$ at atmospheric conditions and phase volumetric flow rates of $\alpha_1 V_1 = 0.2$ to $2\ m/s$, $(1 - \alpha_1) V_2 = 0.2 m/s$, is a slug flow with characteristic slug length of $\ell_{TB} \approx 0.1$ to $0.5m$.

Churn-turbulent flow: In accordance with *Mishima* and *Ishii* (1984) churn-turbulent flow exists under the following conditions:

$$\alpha_1 > \alpha_{1,\text{slug to churn}} \text{ and } \left[\left(D_h < D_{hc} \text{ and } V_1 < V_{11} \right) \text{ or } \left(D_h \geq D_{hc} \text{ and } V_1 < V_{12} \right) \right]. \tag{1.34}$$

Here

$$D_{hc} = \lambda_{RT} / \left[(\alpha_1 - 0.11)^2 N_{\eta 2}^{0.4} \right], \tag{1.35}$$

and

$$N_{\eta 2} = \eta_2 / \sqrt{\rho_2 \sigma_2 \lambda_{RT}} \tag{1.36}$$

is the viscous number. The first criterion is applied to flow reversal in the liquid film section along large bubbles,

$$D_h < D_{hc} \text{ and } V_1 > V_{11}, \tag{1.37}$$

where

$$V_{11} = \left(1 - 0.11/\alpha_1\right) V_{TB}. \tag{1.38}$$

In this case the flow reversal in the liquid film section along the large bubbles causes the transition.

The second criterion is applied to destruction of liquid slugs or large waves by entrainment or deformation

$$D_h \geq D_{hc} \text{ and } V_1 > V_{12}, \tag{1.39}$$

where

$$V_{12} = \frac{V_{2Ku}}{\alpha_1 N_{\eta 2}^{0.2}}, \tag{1.40}$$

and

$$V_{2Ku} = \left[g \sigma_2 \left(\rho_2 - \rho_1\right) / \rho_1^2 \right]^{1/4}, \tag{1.41}$$

is the *Kutateladze* terminal velocity for free-falling droplets in gas. The correlation holds for low viscous flows $N_{\eta 2} < 1/15$ and relatively high liquid *Reynolds* number $\mathrm{Re}_{23} > 1635$. In this case the churn flow bubble section following the slug disintegrates or the liquid waves and subsequent liquid bridges and slugs can be entrained as small droplets. This leads to the elimination of liquid slugs between large bubbles and to a continuous gas core. This is the criterion for transition from slug flow to annular-dispersed flow.

Annular film flow: The annular film flow is defined if

$$\alpha_1 > \alpha_{1,slug\ to\ churn} \text{ and } \left[\left(D_h < D_{hc} \text{ and } V_1 > V_{11} \right) \text{ or } \left(D_h \geq D_{hc} \text{ and } V_1 > V_{12} \right) \right]. \tag{1.42}$$

Annular film flow with entrainment: The annular film flow with entrainment is defined by *Kataoka* and *Ishi* (1982) as follows

$$D_h > D_{hc} \text{ and } \alpha_1 > \alpha_{1,slug\ to\ churn} \text{ and } V_1 > V_{13} \text{ and}$$
$$\mathrm{Re}_{2\delta} = \rho_2 V_2 4\delta_2 / \eta_2 > 160. \tag{1.43}$$

Here $\delta_2 = \frac{1}{2} D_h \left(1 - \sqrt{1-\alpha_2}\right)$ is the film thickness,

$$V_{13} = b_8 \frac{\sigma_2}{\eta_2 \alpha_1 \left(\frac{\rho_1}{\rho_2}\right)^{1/2}}, \tag{1.44}$$

$$b_8 = N_{\eta 2}^{0.8}, \text{ for } \mathrm{Re}_{23} > 1635, \tag{1.45}$$

$$b_8 = 11.78\, N_{\eta 2}^{0.8} / \mathrm{Re}_{23}^{1/3} \text{ for } \mathrm{Re}_{23} \le 1635, \tag{1.46}$$

$$\mathrm{Re}_{23} = \left(1-\alpha_1\right) \rho_2 \left|V_{23}\right| D_h / \eta_2, \tag{1.47}$$

$$V_{23} = \left(\alpha_2 V_2 + \alpha_3 V_3\right) / \left(1-\alpha_1\right). \tag{1.48}$$

1.3.3 Channel flow – inclined pipes

Compared with the vertical flow the flow in horizontal pipes possesses two additional flow patterns – stratified flow and stratified wavy flow. For the computation of the relative velocities and pressure drop for these flow patterns the work by *Mamaev* et al.(1969) is recommended. *Mamaev* et al. considered stratified flow possible for $Fr < Fr_{crit}$, where $Fr = \frac{(\rho w)^2 v_h}{g D_h}$, $v_h = X_1 v_1 + \left(1 - X_1\right) v_2$. The critical *Froude* number was obtained from experiments

$$Fr_{crit} = \left[\left(0.2 - \frac{2\cos\varphi}{\lambda_{fr}}\right) \Big/ \left(1-\beta\right)^2\right] \exp\left(-2.5\beta\right),$$

where $\beta = X_1 v_1 / v_h$, and $\lambda_{fr} = \lambda_{fr}\left(\frac{\pi\left(1-\alpha_1\right)}{\pi - \theta} \frac{w_2 D}{\nu_2}, \frac{k}{D}\right)$ is the liquid side-wall friction coefficient computed using the *Nikuradze* diagram. *Weisman* et al. (1979), *Weisman* and *Kang* (1981), and *Grawford* et al. (1985) published a set of correlations for horizontal as well as vertical flows. Their correlations for horizontal flows are summarized at the end of this section.

Transition criteria are systematically elaborated by *Taitel* and *Dukler* (1976) and *Rouhani* and *Sohal* (1983). The *Taitel* line of criteria development is presented here.

The *Taitel* and *Dukler* (1976) flow map

Stratified flow: Almost all results available in the literature provide a criterion for identification of the existence of stratified flows based on the stability criterion Eq. (2.151b) from Chapter 2 in Volume 1 of this monograph

$$V_{1,stratified} - V_2 = \left[g\cos\left(\varphi - \pi/2\right)\left(\rho_2 - \rho_1\right)\left(\frac{\alpha_1}{\rho_1} + \frac{1-\alpha_1}{\rho_2}\right) \Big/ \frac{d\alpha_2}{d\delta_{2F}} \right]^{1/2}, \quad (1.49)$$

where δ_{2F} is the liquid thickness. φ is the angle defined between the upwards-oriented vertical and the pipe axis – see Fig. 1.8. For a larger velocity difference the flow is no longer stratified and disintegrates into an intermittent flow-like elongated bubble or slug or churn flow. For flow between two parallel plates

$$\frac{d\delta_{2F}}{d\alpha_2} = H\,, \quad (1.50)$$

where H is the distance between the two plates. For flows in a round tube, see Fig. 1.8, the angle θ with the origin at the pipe axis is defined between the upwards-oriented vertical and the liquid-gas-wall triple point as a function of the liquid volume fraction given by the equation

$$1 - \alpha_2 = \frac{\theta - \sin\theta\cos\theta}{\pi}\,. \quad (1.51)$$

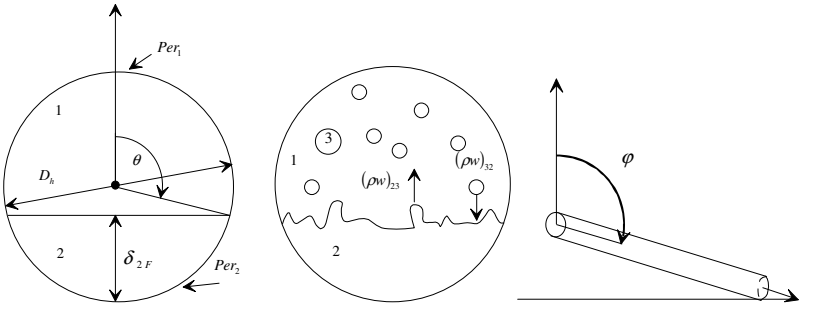

Fig. 1.8 Definition of the geometric characteristics of stratified flow. 1 Gas; 2 continuous liquid (stratified); 3 droplets

Bearing in mind that

$$\delta_{2F} = \frac{1}{2} D_h \left(1 + \cos\theta\right) \quad (1.52)$$

we obtain

$$\frac{d\alpha_2}{d\delta_{2F}} = \frac{d\alpha_2}{d\theta} \Big/ \frac{d\delta_{2F}}{d\theta} = \frac{4}{D_h} \frac{\sin\theta}{\pi} . \tag{1.53}$$

This criterion is in fact consistent with the *Kelvin-Helmholtz* gravity long-wave theory – see *Milne-Thomson* (1968), *Delhaye*, p. 90 (1981), or *Barnea* and *Taitel* (1994).

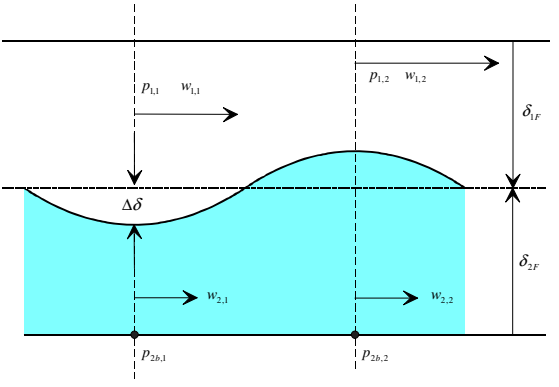

Fig. 1.9 Definition of the variables for the *Hohannessen* stability criterion

Wallis and *Dobson* (1973) compared the above equation with experimental data for channels with H ranging from 0.0254 to 0.305 m and corrected then by introducing a constant multiplier of 0.5. This result was in fact confirmed by *Mishima* and *Ishii* in 1980. These authors obtained for low pressure $\frac{\alpha_1}{\rho_1} >> \frac{1-\alpha_1}{\rho_2}$ the constant 0.487. *Hohannessen* (1972) considered the situation depicted in Fig. 1.9 and defined the transition of the stratified flow as equality of the static pressures at the bottom of the pipe $p_{2b,1}$ and $p_{2b,2}$ taking into account the change of the gas pressure due to cross section decrease by using the *Bernouli* equation. *Taitel* and *Dukler* (1976), similarly to *Hohannessen* (1972), equalized the buoyancy pressure increment required to create solution disturbance with finite amplitude to the increase of the gas dynamic pressure and obtained after linearization the following multiplier $\left(1-\frac{\delta_{2F}}{H}\right)$ again testing the result for low pressure. Defining the *Taylor* bubble velocity for an inclined pipe with

$$V_{TB}^{*} = \left[\frac{\rho_2 - \rho_1}{\rho_2} D_h g \cos\left(\varphi - \pi/2\right) \right]^{1/2} , \tag{1.54}$$

the criterion for a pipe is then

$$V_{1,stratified} - V_2 = \frac{1}{2}(1-\cos\theta)\left[\frac{g(\rho_2-\rho_1)\cos(\varphi-\pi/2)}{\frac{4}{D_h}\frac{\sin\theta}{\pi}}\left(\frac{\alpha_1}{\rho_1}+\frac{1-\alpha_1}{\rho_2}\right)\right]^{1/2} \tag{1.55}$$

or

$$\frac{V_{1,stratified} - V_2}{V_{TB}^*} = \frac{1}{4}(1-\cos\theta)\left[\frac{\pi}{\sin\theta}\rho_2\left(\frac{\alpha_1}{\rho_1}+\frac{1-\alpha_1}{\rho_2}\right)\right]^{1/2}. \tag{1.56}$$

This criterion is valid for gravity-driven liquid flow. *Johnston* (1985) compared the *Taitel* and *Dukler* result and found that the RHS of the above equation has to be multiplied with a factor ranging between 0.39 and 4 with 1 being a good choice. The accuracy of prediction varies from 2% for slow inclinations, 1/10, to 75% for 1/400 inclinations. *Anoda* et al. (1989) confirmed the validity of the above equation for large diameter pipes (0.18 m) and large pressures (3 to 7.3 MPa).

Bestion (1990) reported data for stratification of horizontal flow for a pressure range of 2 to 10 MPa. The data shows that if the liquid velocity is smaller than the bubble free-rising velocity, $V_2 < V_{1Ku}$, the flow is stratified.

Stratified wavy flow: The surface of the liquid remains *smooth* if the gas velocity remains below some prescribed value. *Mamaev* et al. reported in 1969 that waves started within $0.01w_2 \le w_1 \le 3.33w_2$ and are always there for $w_1 > 3.33w_2$. *Taitel* and *Dukler* (1976) derived an approximate expression for the gas velocity exciting waves

$$V_{1,wavy} - V_2 = \left[\frac{4\eta_2 g(\rho_2-\rho_1)\cos(\varphi-\pi/2)}{0.01\rho_2\rho_1 V_2}\right]^{1/2}, \tag{1.57}$$

or after rearranging

$$\frac{V_{1,wavy} - V_2}{V_{TB}^*} = 20\left(\frac{\rho_2}{\rho_1}\right)^{1/2}\left(\frac{\rho_2 V_2 D_h}{\eta_2}\right)^{-1/2}. \tag{1.58}$$

For larger gas velocity the surface of the liquid is *wavy* (stratified wavy flow).

Annular flow – Fig.1.10: The first requirement for the flow to be annular is that the film volume fraction is

$$\alpha_2 < 0.24, \tag{1.59}$$

see *Taitel* (1990), p. 245. More information on the existence of annular flow is contained in the *Weisman-Kang* flow map given below.

Bubble flow: *Taitel* and *Dukler* (1976) investigated gravity-driven flow. The authors found the transition to dispersed bubble flow to occur if the liquid side shear force due to turbulence equals the buoyancy force acting on the liquid. This results in the following criterion

$$V_{2,bubble} - V_2 = \left[\frac{4F}{b} \frac{\alpha_1 g \left(\rho_2 - \rho_1\right) \cos\left(\varphi - \pi/2\right)}{\rho_2 c_{2w}} \right]^{1/2} \tag{1.60}$$

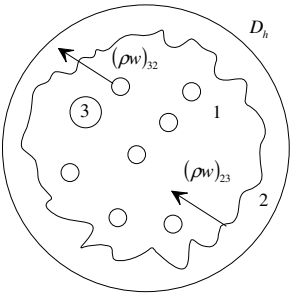

Fig. 1.10 Annular flow: 1 gas, 2 film, 3 droplets

where

$$c_{2w} = \frac{0.046}{\left(\frac{\rho_2 V_2 D_{h2}}{\eta_2} \right)^{1/5}}, \tag{1.61}$$

$$\frac{4F}{b} = 4 \frac{\pi D_h^2 / 4}{D_h \sin\theta} = \frac{\pi}{\sin\theta} D_h . \tag{1.62}$$

F is the pipe cross section and b is the gas-liquid interface median if stratification is assumed. After rearrangement for pipe flow we obtain

$$V_{2,bubble} - V_2 = 8.26 \left[\frac{\alpha_1 D_h g \left(\rho_2 - \rho_1\right) \cos\left(\varphi - \pi/2\right)}{\sin\theta \rho_2} \right]^{1/2} \left(\frac{\rho_2 V_2 D_{h2}}{\eta_2} \right)^{1/10}, \tag{1.63}$$

or

$$\frac{V_{2,bubble} - V_2}{V_{TB}^*} = 8.26 \left(\frac{\alpha_1}{\sin\theta} \right)^{1/2} \left(\frac{\rho_2 V_2 D_{h2}}{\eta_2} \right)^{1/10} . \tag{1.64}$$

For smaller gas velocities bubble flow exists. For larger gas velocities flow is in the intermittent regime.